Research Square

Preprints are preliminary reports that have not undergone peer review.
They should not be considered conclusive, used to inform clinical practice,
or referenced by the media as validated information.

Hydroxysafflor yellow A promotes osteogenesis and bone development via epigenetically regulating β-catenin and prevents ovariectomy-induced bone loss

Peng Wang
Guangzhou University of Chinese Medicine
Wang Min
Guangzhou University of Chinese Medicine
Tingling Zhuo
Guangzhou University of Chinese Medicine
Ying Li
Guangzhou University of Chinese Medicine
Lin Weiping
Chinese University of Hong Kong
Ding Lingli
Guangzhou University of Chinese Medicine
Meng Zhang
Guangzhou University of Chinese Medicine
Chi Zhou
Guangzhou University of Traditional Chinese Medicine First Affiliated Hospital
Jinfang Zhang
Guangzhou University of Chinese Medicine
Gang Li
Chinese University of Hong Kong
Haibin Wang
Guangzhou University of Traditional Chinese Medicine First Affiliated Hospital
Liangliang Xu (xull-2016@gzucm.edu.cn)
Guangzhou University of Chinese Medicine https://orcid.org/0000-0002-5249-7480

Research

Keywords: Hydroxysafflor yellow A, osteoporosis, KDM7A , β catenin

Posted Date: November 24th, 2020

DOI: https://doi.org/10.21203/rs.3.rs-38205/v2

License: This work is licensed under a Creative Commons Attribution 4.0 International License.
Read Full License

Version of Record: A version of this preprint was published at The International Journal of Biochemistry & Cell Biology on August 1st, 2021. See the published version at https://doi.org/10.1016/j.biocel.2021.106033.

Hydroxysafflor yellow A promotes osteogenesis and bone development via epigenetically regulating β-catenin and prevents ovariectomy-induced bone loss

Peng Wang[1#], Min Wang[1#], Tingling zhuo[1], Ying Li[1], Weiping Lin[2], Lingli Ding[1], Meng Zhang[1], Chi Zhou[3,4], Jinfang Zhang[4], Gang Li[2], Haibin Wang[3,4*], Liangliang Xu[3,4*]

[1]Guangzhou University of Chinese Medicine, Guangzhou, China.

[2]Department of Orthopaedics and Traumatology, Faculty of Medicine, Prince of Wales Hospital, The Chinese University of Hong Kong, Shatin, Hong Kong, China.

[3]Department of Joint Orthopaedics, the First Affiliated Hospital, Guangzhou University of Chinese Medicine, Guangzhou, Guangzhou, China.

[4]Laboratory of Orthopaedics & Traumatology, Lingnan Medical Research Center, Guangzhou University of Chinese Medicine, Guangzhou, China.

[#]Contributed equally as first authors.

[*]Contributed equally as corresponding authors.

Correspondence

Liangliang Xu, PhD., The First Affiliated Hospital of Guangzhou University of Chinese Medicine, Guangzhou University of Chinese Medicine, Guangzhou, China. Tel: (86) 20-36585574, E-mail: xull-2016@gzucm.edu.cn; Dr. Haibin Wang, Guangzhou University of Chinese Medicine, Jichang Road, Baiyun District, Guangzhou, China. Tel: (86) 20-84237212, E-mail: hipknee@163.com.

Abstract

In clinical treatment, there is increasingly prevalent that traditional Chinese medicine treats common bone diseases including osteoporosis. Hydroxysafflor yellow A (HSYA), one of the essential compounds of Safflower, has strong effects to scavenge oxidative stress and inhibit apoptosis. It has been used as the therapy for thrombus, myocardial ischemia, and inflammation, but its effect on osteoporosis has not been explored. In this study, we found HSYA could enhance the cell viability and promote osteogenesis of hBMSC in vitro. Mechanistically, HSYA could increase the expression of β-catenin leading to its accumulation in the nucleus and activation of down-stream targets to promote osteogenesis. In addition, RNAseq and quantitative RT-PCR showed KDM7A was significantly increased by HSYA. The occupancy of H3K27me2 on β-catenin promoter was significantly decreased by HSYA, which could be reversed by silencing endogenous KDM7A. More importantly, HSYA could promote bone development in chick embryos and prevent ovariectomy (OVX)-induced bone loss in SD rats. Taken together, our study has shown convincing evidence that HSYA can promote osteogenesis and bone development via epigenetically regulating β-catenin and prevents ovariectomy-induced bone loss. HSYA might be used to treat some skeletal diseases such as osteoporosis.

Keywords

Hydroxysafflor yellow A, osteoporosis, KDM7A, β-catenin

Introduction

Bone is a complex tissue which protects various soft tissues and maintains the mineral metabolism in the microenvironment [1]. MSCs (mesenchymal stem cells) derived from bone marrow or other tissues are capable of self-replication and have multiple differentiation potentials, including osteoblast and adipocyte. Osteogenesis and adipogenesis of MSCs are strictly regulated under various physiological signal transduction pathways to maintain a dynamic balance. The ability to form adipocytes from MSCs will be inhibited when MSCs differentiate to osteoblasts, and vice versa [2]. Therefore, excessive adipocytes have been proven to be the pathogenesis of several bone disorders, including osteoporosis [3], which may be related to bone loss.

Wnt/β-catenin and TGF-β/BMPs/Smads pathways play key roles in the osteogenic differentiation of MSCs. β-catenin, Runx2, and PPARγ are important transcription factors for MSCs to differentiate into osteoblasts and adipocytes [4]. Wnt/β-catenin pathway can mediate more than 50 type's proteins which are able to stimulate biological responses of various cells. The key switch in the canonical Wnt pathway is the cytoplasmic protein β-catenin [5]. Wnt protein acts on β-catenin's cell-surface receptor to prevent β-catenin degradation. Then, the up-regulated β-catenin can translocate into the nucleus and stimulate the expression of different down-stream genes. β-catenin is required for MSCs to differentiate into either osteoblasts or chondrocytes during the early stages of fracture repair [6,7]. The researchers created a type of mice with β-catenin depletion in the osteoblast lineage through using alpha 1 type 1 collage-Cre (Col1a1-Cre) mice. They found that mice with β-catenin depletion present a low bone mass phenotype because of increased osteoclastic bone resorption due to decreased expression of

osteoprotegerin (OPG) [8].

Multiple experimental studies have shown that epigenetic factors are involved in the process of bone growth, regeneration, and repair. This process includes the dynamic balance of osteoblast and adipocyte regulation. Our previous studies have demonstrated that epigenetic regulations such as DNA methylation and histone methylation are involved in the differentiation and migration of bone marrow-derived MSCs (BMSCs) [9], and the incidence of osteoporosis [10]. Moreover, there is a specific connection between β-catenin and epigenetics in osteogenesis. MiR-29a can regulate the acetylation of β-catenin, which directly influences the activity of osteoblast cultures [11]. Histone methyltransferase SETD2 regulates osteosarcoma cell growth and chemosensitivity by suppressing Wnt/β-catenin signaling [12]. Knocking-down β-catenin reduced EZH2 (a key component of the PRC2 complex that catalyzes histone methylation) protein levels and H3K27me3 at osteogenic loci [13]. Our previous research showed that lncRNA H19 can promote osteoblast differentiation by regulating Wnt/β-catenin pathway through acting as a competing endogenous RNA in hMSCs [14].

Safflower, known as *Carthamus tinctorius L***,** has already been applied in various medical fields such as digestology, anesthesiology, and infectious immunology for antipyretic substances and purgative, analgesic [15]. Our previous studies have shown Huo Xue Tong Luo capsule (HXTL capsule) containing *Safflower, Angelica sinensis* etc, could promote osteogenesis and prevent the development of osteonecrosis [16,17]. Hydroxysafflor yellow A (HSYA) is an active compound isolated from *Safflower* which has strong effects to scavenge oxidative stress and inhibit apoptosis. It has been widely used as the therapy for thrombus, myocardial ischemia, and inflammation [18]. It is also reported that HSYA can enhance the

formation of E-cadherin/β-catenin complex by inhibiting adhesion, invasion, migration, and lung metastasis of hepatoma cells [19]. Moreover, previous studies showed that HSYA has biological effects on the prevention of osteoarthritis and proliferation and differentiation of 3T3-L1 preadipocytes [20,21]. However, its effects on osteogenesis of MSCs as well as osteoporosis prevention have not been explored.

In the present study, we focused on the potential effects of HSYA on the osteogenesis of hBMSCs and the underlying mechanism in vitro, as well as in vivo investigations on its beneficial effects on bone development in chick embryos and the prevention of ovariectomy (OVX)-induced osteoporosis rat model.

Materials and methods

Chemicals and antibodies

HSYA (purity>98% by HPLC; Fig. 1A) was purchased from Weikeqi Biological Technology Corporation (Sichuan, China), and dissolved in dimethyl sulfoxide (DMSO; Sigma - Aldrich, Australia) to a concentration at 20mM for storage. Fertilized Leghorn eggs were obtained from the Avian Farm of the South China Agriculture University (Guangzhou, China). Modified Eagle's Medium of Alpha (α-MEM), fetal bovine serum (FBS), and penicillin/streptomycin were purchased from Gibco (USA). β-glycerolphosphate, dexamethasone, and ascorbic acid phosphate were purchased from Sigma (USA). Alizarin RED S was purchased from Solarbio (Beijing, China). Cell Counting Kit-8 (CCK-8) and BCIP/NBT alkaline phosphatase coloration kit were purchased from Beyotime (Beijing, China). Lipofectamine 3000 transfection reagent

was obtained from Thermo (USA). Takara Mini BEST Universal RNA Extraction Kit, Prime Script RT Master Mix (Perfect Real Time) and SYBR-Green Master Mix were supplied by Takara (Japan). Trizol reagent was obtained from Invitrogen (USA). Polyvinylidene difluoride (PVDF) membrane was obtained from Millipore (USA). Primary antibodies against Runx2, H3K9me2 and DAPI were supplied by Cell Signaling Technology (USA); Primary antibodies against β-catenin and anti-OPN were purchased from Bioworld (USA); Anti-Osterix, anti-Runx2, anti-BMP2, anti-GAPDH, and anti-H3K27me2 antibodies were obtained from Abcam (USA). Secondary antibodies (HRP-conjugated Goat Anti-Rabbit IgG) were obtained from Abcam (USA). ChIP-Grade Protein G Magnetic Beads were donated from Cell Signaling (CST, USA). Dual-Luciferase Reporter Assay System was supplied by Promega Company (USA).

Cell culture

Human bone marrow-derived MSCs (hBMSCs) were donated from the Cyagen Biosciences Corporation (USA) in the Guangzhou, China. The cells were kept in α-MEM supplemented with 10% FBS and 1% penicillin/streptomycin. The surface antigens of hBMSCs clusters were detected through flow cytometry by the biological company. The hBMSCs between passage 2 and 8 were used in this study.

Cell viability assay

The effect of HSYA on the proliferation of hBMSCs was assessed using CCK-8 kit. In brief, an initial density of 5×10^3 cells/well were prepared in 96-well plates and cultured in a graded series of HSYA for 1, 2, and 3 days. For the H_2O_2 stress model, BMSCs were treated with different

concentrations of H_2O_2 (0-600 μM) for 2h, then HSYA was added for another 24h. Subsequently, 20μl CCK-8 solution and 180μl culture media were added to each well at the respective time point and the plates were incubated for 4 h at 37°C. 100μl aliquots were taken from each well and transferred to another 96-well plate for final analysis. The absorbance of the samples was measured at 450 nm with a spectrophotometric micro plate reader (Xianke Instruments, Shanghai, China).

Western blotting

Equal proteins were loaded onto 8% SDS-PAGE and subsequently transferred onto a PVDF membrane for 120 min at 350mA. The membrane was blocked with 5% skim milk for 1 h at room temperature. After washing 3 times with TBS containing 0.1% Tween 20 (TBST), the membranes were incubated, respectively, with anti-Runx2 (1:1000), anti-β-catenin (1:1000), or anti-GAPDH (1:1000) antibodies at 4°C overnight. After washing in TBST for 3 times (5 min for each time), the membrane was incubated with horseradish peroxidase-linked secondary antibodies (anti-rabbit) for 2 h at room temperature. After washing five times with TBST, proteins were detected with ECL western blotting detection reagent (Beyotime, China) according to the manufacturer's instructions.

Osteogenic induction assay and ALP staining

To induce osteogenic differentiation, the culture media were replaced with osteogenic induction medium when cells reached a confluence of over 70%. The media were changed every 2 days. The hBMSCs were treated with or without OIM (osteogenic induction medium) containing α-

MEM supplemented with 20mM β-glycerophosphate, 100nM dexamethasone, and 50μM ascorbic acid phosphate and HSYA for 7 days before the cells were washed with PBS twice and fixed with 70% ethanol for 10 min. The cells were incubated with BCIP/NBT alkaline phosphatase coloration kit at 37°C for 1 h. Then the reaction was stopped by distilled water and the plate was dried before taking photo.

Mineralization assay

After 14 days of osteogenic induction, cells were fixed and stained with 0.5% Alizarin Red S (pH 4.1) for 10 min. Then washed three times with deionized water. The calcium deposition was extracted with 10% cetylpyridinium chloride and quantified by measuring the OD550 nm.

RNA extraction and real-time PCR

Total RNA was extracted from cultured hBMSCs using Takara Mini BEST Universal RNA Extraction Kit according to the manufacturer's instructions. Briefly, the cells were lysed with Buffer RL reagent for 10 min. DNase I was used to remove contaminating DNA in total RNA. The first-strand cDNA was synthesized using Prime Script RT Master Mix (Perfect Real Time). Real-time PCR was performed using the CFX96 Real-Time PCR Detection System (Bio-Rad, USA). The reaction conditions consisted of 15ul reaction volumes with diluted cDNA template 2μl, 7.5μl SYBR-Green Master Mix (2×), 4.5ul PCR-Grade water and 0.5ul of each primer (10μM). Amplification conditions were as follows: first at 95°C for 5 min, and then 45 cycles of 95°C for 15s and 60°C for 60s. Primer sequences were listed in **Supplementary Table 1**. The relative quantification of gene expression was normalized to the expression level of β-actin.

RNA sequencing

hBMSCs treated with 10μM HSYA for 7 days or not were used for RNA sequencing (RNA-seq) analysis. The cells were washed with PBS for three times and collected by TRIzol Reagent. The quality and integrity of total RNA samples were assessed using a 2100 Bioanalyzer or a 2200 TapeStation (Agilent Technologies) according to the manufacturer's instructions. The preparation of whole transcriptome libraries and deep sequencing were performed by the Annoroad Gene Technology Corporation (Beijing, China). DAVID and KOBAS bioinformatics tools were used for functional annotation enrichment and clustering. The changed genes in RNAseq data are listed in **Data file S1**.

Cell transfection

The sequences of each siRNA targeting human KDM7A were listed in **Supplementary Table 2**. The siRNA transfection was performed with Lipofectamine 3000 transfection reagent according to the manufacturer's instructions. Briefly, hBMSCs were plated in α-MEM medium into 12-well plate, and allowed to reach 50–60% confluency. Two days later the total RNA was extracted for real time PCR analysis.

Luciferase reporter assays

Experiments were conducted as mentioned before [22]. In brief, HEK293 cells were seeded on a 24-well plate, and the cells were allowed to grow until 80% confluency. Cells were then transfected with TOPflash (500ng) and Renilla reporter plasmid pRL‐CMV (100ng) by using

Lipofectamine 3000. Twenty‐four hours after transfection, cells were treated with HSYA in different concentrations for 24 hours. The luciferase activity was measured using GloMax™20/20 Single tube luminometer (Promega, Madison, WI, USA).

Cell immunofluorescence

hBMSCs were collected after 24h of 10μM treatment, and inoculated into 24-well plates with 5×10^3 cells /ml, getting ready for slide climbing. After 4 hours, the cells were fixed with 4% paraformaldehyde for 30 min. 5%BSA was added to the slides and sealed at room temperature for 30min. β-catenin antibody (1:200) or H3K27me2 antibody (1:200) or H3K9me2 antibody (1:200) was added to the sealant and incubated overnight at 4°C. After drying the excess liquid on the slides, fluorescent secondary antibody (1:500) was added and incubated in the wet box at room temperature for 1h. DAPI was used to dye the core, and the cover glass was used to seal the sample for development and photography.

Chromatin immunoprecipitation assay

Cross-linking and chromatin immunoprecipitation (ChIP) were done as described previously [23]. Briefly, all of the subsequent steps were performed at 4°C, and all buffers contained 0.1mM EDTA, 0.5mM EGTA, 1mM dithiothreitol, and protease inhibitors (BD). The hBMSCs were washed with phosphate-buffered saline (pH 7.4) and lysed. After centrifugation, the pellet was resuspended in 10 ml of 10mM Tris-HCl, pH 8.0, and 200mM NaCl; centrifuged at 15,000g for 15 min. The chromatin pellet was resuspended in 1 ml of 50mM Tris-HCl, pH 7.9, and 5mM CaCl2 and digested with 500 units of micro coccal nuclease (New England Biolabs) at 37 °C

for 10 min. For ChIP reactions, the samples (1 ml) were immunoprecipitated overnight with anti-H3K9me2, H3K27me2, or control rabbit IgG. ChIP-PCR analysis was done by using 3 μl of ChIP DNA and the primer sequence was shown as follows: sense: ATTAGCAAAGAATCACCC; anti-sense: TGAACAAACCAAAGACAG. The enrichment was determined relative to a control ChIP with IgG antibody.

Embryo manipulation

Fertilized Leghorn eggs were incubated in a humidified incubator (Jinweng Instruments, Shanghai, China) at 37°C until the embryos reached the desired developmental stage [24]. The chick embryos were exposed to HSYA (10μM) or PBS in equal volume for 14 days. In brief, 200μl PBS including DMSO or 10μM HSYA were carefully injected into a small hole made in the air chamber of the egg on 2 days of incubation. After the treatment, the embryos were further incubated for 14 days before being harvested for analysis.

Alcian blue and Alizarin Red S staining of chicken skeleton

To visualize the skeleton, the chick embryos were stained with alcian blue and alizarin red dyes as described [25]. Fifteen-day-old chick embryos were fixed in 95% ethanol for 2 days with the fur and skin and viscera carefully removed, and then the specimens were post-fixed in the mixture solution (100% ethanol/acetic acid/saturated Alcian blue in 75% ethanol, 20:5:3) for two days. The embryos were stained in saturated Alizarin Red S (Solarbio, Beijing, China) in ultrapure water / 1% KOH dye for 1 week and then in 25% glycerol / 1% KOH for clearing lasting 2 days. Finally, the embryos were treated with a graded series (50%-75%-100%) of

glycerol for 5 days, respectively. To make parts of the skeleton more visible, we carefully dismembered long bone tissues and photographed them using a stereomicroscope (Ckx41 Olympus, German). The length of the alizarin red stained portion of each spine, radius, and metatarsus were quantified and analyzed using the Image J software.

Ovariectomy (OVX)-induced osteoporosis rat model

Twenty-four SD rats (females; 280-320g, 16 weeks old) were supplied by the Animal Experiment Center of Guangzhou University of Chinese Medicine. The rats were placed in the First Affiliated Hospital of Guangzhou University of Chinese Medicine (Approval No. TCMF1-2018011). All rats were randomly divided into four groups: sham group (n=6), OVX group (n=6), OVX+HSYA (2.5mg/kg) group (n=6) and OVX+HSYA (10mg/kg) group (n=6). Bilateral ovariectomies were performed to induce osteoporosis under general anesthesia for OVX and OVX+HSYA groups. For the sham group, the ovaries were only exteriorized but not resected. All rats had 3 days recovery after the operation, and then an intraperitoneal injection of HSYA (2.5mg/kg&10mg/kg, every 2-3 days for 12 weeks) was delivered to OVX +HSYA group. The sham and OVX group mice were intraperitoneally injected with PBS as a vehicle control.

Micro-CT analysis

After sacrificing the experimental rat groups, the right tibia (n=6 for each treatment group) were fixed with 4% paraformaldehyde (PFA) for 24 hours and placed in 5 ml centrifuge tubes and scanned using Skyscan 1176 micro-CT scanner (Bruker micro-CT, Kontich, Belgium). The

scanning was carried out using the following settings: voltage, 50 kV; source current, 500 μA; Al 0.5 mm filter; pixel size 27 μm; rotation step, 0.4 degree. Cancellous bone of the proximal tibia 2.7 mm above the growth plate was chosen as the VOI, which was restricted to an internal region of the femur where trabecular and cortical bones were extracted by drawing free form contours with the CT analyzer software. The bone volume/tissue volume (BV/TV), mean volumetric bone mineral density (BMD), trabecular number (Tb. N), trabecular thickness (Tb. Th) and trabecular separation (Tb. Sp) were measured. Twoand three-dimensional images were generated using Data-viewer and CTvol softwares (Bruker micro-CT, Kontich, Belgium) respectively.

Histological and immunohistochemical analysis

The samples were washed in PBS, fixed in 4% paraformaldehyde, decalcified, dehydrated, and embedded in paraffin. The sections were cut at a thickness of 5 μm and stained with hematoxylin and eosin (H&E) after deparaffination. As for immunohistochemical (IHC) analysis, primary antibodies against β-catenin (1:200), Runx2 (1:200), OPN (1:200) and BMP2 (1:200), and goat anti-rabbit or mouse IgG horseradish peroxidase (HRP)-conjugated secondary antibodies were used for detection. Images were acquired with the Aperio ScanScope (Leica Biosystem, Buffalo Grove, IL, USA).

Statistical analysis

All data and statistical analysis were followed with the recommendation of pharmacology experimental design. All quantitative data was analyzed by a commercially available statistical

program SPSS version 20.0 (IBM, USA). The two-tailed Student's t-test was applied for comparisons of two groups and one-way analysis of variance (ANOVA) with the Tukey' post hoc test for three or more groups. $P<0.05$ as considered statistical significance. All data were presented as mean ± SD.

Results

HSYA enhanced the proliferation of hBMSCs

The basic chemical structure of HSYA was shown in **Fig. 1A.** To investigate the effect of HSYA on cell viability, the CCK-8 assay was performed. The result showed that the proliferation of hBMSCs was increased by HSYA at 10μM, especially at Day 3 (**Fig. 1B**). When BMSCs were treated with different concentrations of H_2O_2 (0–600 μM) for 2 h, the cell viability assay showed 600 μM was the best concentration for H_2O_2 stress model (**Fig. 1C**). Then the cells were challenged with 600 μM H_2O_2, HSYA at the concentration of 10μM could significantly improve the viability of BMSCs (**Fig. 1D**).

HSYA promoted osteogenesis of hBMSCs

To investigate the role of HSYA on osteogenesis of MSCs, hBMSCs were cultured in OIM with or without HSYA at various concentrations (0, 1, 10, 20, and 40μM) for 7 days. Then the cells were fixed and stained with BCIP/NBT alkaline phosphatase coloration kit. The result showed HSYA, particularly at the concentration of 10μM, could significantly increase the ALP activity of hBMSCs (**Fig. 2A**). Therefore, the hBMSCs were treated with OIM for 14 days to visualize

the formation of calcium deposits stained by Alizarin Red S. We observed that HSYA significantly increased the formation of calcium deposits, and reached the peak value at the dosage of 10μM (**Fig. 2B&C**). Then we further checked the expression of osteogenesis-related genes in hBMSCs treated with various doses of HSYA. The quantitative real time PCR result showed that the RNA levels of OPN, OPG, Runx2 and Col1a1 were significantly up-regulated by HSYA at 10μM (**Fig. 2D**). Since Runx2 is a master transcription factor governing osteogenesis of MSCs, we also evaluated the protein level of Runx2 by western blot. The result showed that Runx2 level was significantly increased by HSYA at different doses (**Fig. 2E&F**). Based on these results, we concluded that 10μM HSYA was the most suitable dosage that could be used to promote osteogenesis of hBMSCs.

HSYA activated Wnt/β-catenin signaling pathway in hBMSCs

It is well known that Wnt/β-catenin signaling pathway is one of the most important signaling pathways in regulation of osteogenic differentiation of MSCs. In order to check whether Wnt/β-catenin signaling pathway was activated or not when hBMSCs were treated with HSYA, we performed quantitative real time PCR and western blotting to detect the level of β-catenin in hBMSCs. The result showed that β-catenin was significantly up-regulated in hBMSCs when they were treated with 10μM HSYA (**Fig. 3A-C**). In addition, we also used the TOPflash assay to evaluate the effect of HSYA on the activation of Wnt/β-catenin signaling pathway. As shown in **Fig. 3D&E**, after 24-hour stimulation, the luciferase activity was significantly increased by HSYA at the dosage of 10μM. Moreover, cell immunofluorescence was undertaken to evaluate the successful nucleus translocation of β-catenin, which is tightly associated with the activation

of the Wnt/β-catenin signaling pathway. It is found that the level of β-catenin (stained with red color) in the nucleus of the hBMSCs treated with HSYA was much higher than that of the control group (**Fig. 3F**).

HSYA activated β-catenin expression via KDM7A mediated histone demethylation

To further explore the underlying mechanism leading to the increase of β-catenin, RNA sequencing was used to analyze the changes of genes in hBMSCs treated with 10μM HSYA. The Heatmap and Volcano map were shown in **Fig. 4A&B**. Among the significantly changed genes, we found many genes of KDM family involved in demethylation of specific methyl markers were differentially expressed (**Fig. 4C**). As confirmed by qPCR analysis, we found KDM7A was the most conspicuous one (**Fig. 4D**). It is well known that KDM7A is a histone demethylase specifically demethylates dimethylated 'Lys-9' and 'Lys-27' (H3K9me2 and H3K27me2, respectively) of histone H3, so we wonder whether KDM7A plays an epigenetic role in regulating the expression of β-catenin. We compared the levels of H3K9m2 and H3K27m2 (repressive histone modifications) in hBMSCs after 10μM HSYA interference by confocal microscopy. The fluorescein could be identified in cell nucleus and the 10μM HSYA-treated groups showed significantly darker signal of H3K9m2 and H3K27m2, respectively **(Fig. 4E&F).** Furthermore, siRNAs targeting KDM7A were designed and transfected into hBMSCs to silence endogenous KDM7A expression **(Fig. 4G)**. The most effective one was chosen to check whether knockdown KDM7A would reverse the influence of HSYA on the binding of H3K9m2 and H3K27me2 on the promoter of β-catenin. The chromatin immunoprecipitation (ChIP)-PCR assay demonstrated the occupancy of H3K27me2 on the promoter region of β-

catenin was significantly decreased by HSYA, but the binding of H3K9me2 was not distinctly different comparing with that of control group, and the effect of HSYA on histone modifications could be reversed by silencing KDM7A **(Fig. 4H&I)**. Taken together, these results showed that HSYA could promote osteogenesis through KDM7A mediated H3K27m2 demethylation on the promoter of β-catenin leading to increased β-catenin expression.

HSYA exposure accelerated endochondral ossification during chick embryo development

According to the results above, we further conducted the chick embryo model to evaluate whether HSYA can accelerate bone development of chick embryos. The chick embryos were exposed to HSYA (10μM) or PBS in equal volume for 14 days. The spine, radius, and metatarsus were then examined using Alcian blue and Alizarin Red S double staining **(Fig. 5A).** The length of the radius stained with Alizarin Red was measured between control and HSYA treated groups and statistically analyzed (PBS: 70.78$\pm$25.89 mm; HSYA: 105.70$\pm$14.09 mm; n=12 for each group). For the femur, the extent of staining was PBS: 64.53$\pm$22.15mm; HSYA: 90.63$\pm$27.53 mm (**Fig. 5B**). These results implied that HSYA exposure during embryogenesis significantly accelerates bone mineralization.

HSYA prevented OVX-induced bone loss in SD rats

Having established that HSYA has an effect on enhancing bone formation in vitro and in vivo, we then investigated whether HSYA could be used to prevent OVX-induced osteoporosis. The SD rats were OVX- or sham-operated and then injected with HSYA (2.5mg/kg or 10mg/kg) or PBS every 2 days for 12 weeks post-surgery. The femurs were collected for Micro-CT and

histological analysis. The Micro-CT analysis showed that the low dose HSYA was much better than the high dose group in preventing the extensive bone mass loss in the OVX rat model (**Fig. 6A**). The bone parameters including BMD, BV/TV, Tb.N and Tb.Th were significantly increased and Tb.Sp was significantly decreased in the low dose HSYA group (2.5mg/kg) (**Fig. 6B**). The H&E staining result also showed the improved trabecular structure in groups treated with HSYA (**Fig. 7**). Immunohistochemistrical staining showed that HSYA significantly stimulated the expression of β-catenin, Runx2, OPN and BMP2 in the trabecular bone, and 2.5mg/kg HSYA showed better effects (**Fig. 7**).

Discussion

In this study, we demonstrated that HSYA enhance osteogenic effect of hBMSCs through KDM7A mediated histone demethylation on β-catenin promoter in vitro. In vivo, HSYA could promote skeletal development in chick embryos and maintain the bone matrix in the OVX rat model.

Bone is a kind of tissue remodeled constantly. Under certain pathological conditions, an imbalance between bone resorption and bone formation may occur, leading to abnormal bone remodeling and the development of bone diseases such as osteoporosis. Clinically, this manifests as age-related osteoporosis associated with bone loss and increased fat accumulation [26].

MSCs which can be easily cultured and expanded are able to multi-directionally differentiate into various cells. However, the ability of MSCs to differentiate into functional osteoblasts is still limited in vivo [27]. The main reason is the adipogenic tendency of the

precursor cell can suppress the tendency of osteogenic differentiation, and then breaks this bidirectional balance to cause osteoporosis [28]. Once osteoblast differentiation is abnormal, it will have an important impact on bone metabolism balance. On the other hand, osteoclasts responsible for bone resorption evolve from the lineage of monocytes differentiated from hematopoietic stem cells, and their differentiation process is also regulated by a variety of factors. Multiple studies have shown that the expression of PPARγ, C/EBPα and C/EBPβ in hematopoietic cells are essential for activating osteoclast differentiation and maturation, and can directly affect the osteoclastogenesis process of hematopoietic stem cells [29-31]. This indicates that adipogenic differentiation of MSCs can directly promote osteoclastogenesis and bone resorption by breaking the coupling balance between osteoblasts and osteoclasts, which in turn leads to the occurrence of osteoporosis. Therefore, promoting the osteogenic differentiation of MSCs and inhibiting their adipogenic differentiation to correct the imbalance of bone metabolism is one of the directions for the treatment of osteoporosis.

In the present study, we have evaluated the effect of HSYA on osteoblastic differentiation of hBMSCs. We showed that HSYA could increase ALP activity, an early osteogenic marker, which can stimulate calcium to form hydroxyapatite and then promote mineralization [32]. This was further confirmed by Alizarin Red S staining. Runx2 is a master transcriptional factor of osteogenesis. It has been demonstrated that osteoblast differentiation normally occurs in $Runx2^{+}OSX^{-}$ mesenchymal cells, while in Runx2-deleted embryos, osteoblast differentiation is inhibited [33]. We found that it was significantly increased by HSYA in hBMSCs. It is reported that Wnt/β-catenin signaling directly enhances Runx2 through both canonical and non-canonical pathways, leading to bone formation ultimately [34]. Our results showed that HSYA

could promote osteogenic differentiation of hBMSCs through activating β-catenin. In addition, RNA-sequencing analysis was used for the exploration of the mechanisms underlying the effects of HSYA. Among the differentially changed genes, we noticed six KDMs orthologous genes were significantly changed by HSYA. We proved that KDM7A mediated histone demethylation on the promoter region of β-catenin was responsible for its activation. KDM7A has been proved to remove di-methylation marks of histone H3K9 and H3K27 [35]. Previous researches reported that KDM7A can suppress tumors through blocking tumors growth and angiogenesis, and regulate neural differentiation and fibroblast growth factor-4 (FGF-4) expression. The effects of H3K27me2/H3K9me2 on regulating osteogenic differentiation are investigated in recent years, and H3K9me2 is supposed to be concluded that it may have the impact on differentiation of hBMSCs [36,37].

Furthermore, we also evaluated the biological function of HSYA in accelerating the mineralization of bone in chick embryos. It was clearly demonstrated by the extent of calcification of the spine, radius, metatarsus and femur, which proved the promoting effect of HSYA on bone development, and in accordance with osteogenic ability of HSYA in hBMSCs. Finally, we established an OVX rat model to further investigate whether HSYA has potential therapeutic effect in vivo. The results showed that HSYA exhibited a remarkable protective effect on OVX-induced osteoporosis in a rat model as confirmed by micro-CT and histological and immune-histochemical analysis. This finding is consistent with the previous report that HSYA could inhibit bone resorption and reverse glucocorticoid induced bone loss in zebrafish [38].

In conclusion, our study has demonstrated that HSYA can accelerate osteogenesis of

hBMSCs via histone demethylation mediated by KDM7A, and β-catenin is likely to be one of important targets of KDM7A which further leads to the expression of downstream osteogenesis-related genes. More importantly, HSYA is capable of promoting bone development and suppressing ovariectomized osteoporosis. These findings could pave the way to the development of HSYA-targeted therapeutic treatments for skeletal diseases such as osteoporosis.

Acknowledgement

The work was supported by grants from National Natural Science Foundation of China (NSFC No. 81871778, 81774339), Guangdong Provincial Science and Technology Project (No. 2017A050506046). The funding institutions had not any role in study design, data collection, data analysis, interpretation nor writing of the report in this study.

Conflict of interests

The authors declare that they have no competing interests.

References:

1. Cohen MM, Jr. The new bone biology: pathologic, molecular, and clinical correlates. American journal of medical genetics Part A 2006;140(23):2646-706.
2. Yousefi AM, James PF, Akbarzadeh R, Subramanian A, Flavin C, Oudadesse H. Prospect of Stem Cells in Bone Tissue Engineering: A Review. Stem Cells Int 2016;2016:6180487.

3. Takada I, Kouzmenko AP, Kato S. Molecular switching of osteoblastogenesis versus adipogenesis: implications for targeted therapies. Expert Opin Ther Targets 2009;13(5):593-603.

4. Huang W, Yang S, Shao J, Li YP. Signaling and transcriptional regulation in osteoblast commitment and differentiation. Front Biosci 2007;12:3068-92.

5. Nusse R, Clevers H. Wnt/beta-Catenin Signaling, Disease, and Emerging Therapeutic Modalities. Cell 2017;169(6):985-99.

6. Day TF, Guo X, Garrett-Beal L, Yang Y. Wnt/beta-catenin signaling in mesenchymal progenitors controls osteoblast and chondrocyte differentiation during vertebrate skeletogenesis. Dev Cell 2005;8(5):739-50.

7. Chen Y, Whetstone HC, Lin AC, Nadesan P, Wei Q, Poon R, et al. Beta-catenin signaling plays a disparate role in different phases of fracture repair: implications for therapy to improve bone healing. PLoS Med 2007;4(7):e249.

8. Holmen SL, Zylstra CR, Mukherjee A, Sigler RE, Faugere MC, Bouxsein ML, et al. Essential role of beta-catenin in postnatal bone acquisition. J Biol Chem 2005;280(22):21162-8.

9. Chen R, Lee WY, Zhang XH, Zhang JT, Lin S, Xu LL, et al. Epigenetic Modification of the CCL5/CCR1/ERK Axis Enhances Glioma Targeting in Dedifferentiation-Reprogrammed BMSCs. Stem Cell Reports 2017;8(3):743-57.

10. Wang P, Cao Y, Zhan D, Wang D, Wang B, Liu Y, et al. Influence of DNA methylation on the expression of OPG/RANKL in primary osteoporosis. Int J Med Sci 2018;15(13):1480-85.

11. Ko JY, Chuang PC, Chen MW, Ke HC, Wu SL, Chang YH, et al. MicroRNA-29a ameliorates glucocorticoid-induced suppression of osteoblast differentiation by regulating beta-catenin acetylation. Bone 2013;57(2):468-75.

12. Jiang C, He C, Wu Z, Li F, Xiao J. Histone methyltransferase SETD2 regulates osteosarcoma cell growth and chemosensitivity by suppressing Wnt/beta-catenin signaling. Biochemical and biophysical research communications 2018;502(3):382-88.

13. Sen B, Paradise CR, Xie Z, Sankaran J, Uzer G, Styner M, et al. β-Catenin Preserves the Stem State of Murine Bone Marrow Stromal Cells Through Activation of EZH2. Journal of bone and mineral research : the official journal of the American Society for Bone and Mineral Research 2020;35(6):1149-62.

14. Liang WC, Fu WM, Wang YB, Sun YX, Xu LL, Wong CW, et al. H19 activates Wnt signaling and promotes osteoblast differentiation by functioning as a competing endogenous RNA. Scientific reports 2016;6:20121.

15. Kim JH, He MT, Kim MJ, Yang CY, Shin YS, Yokozawa T, et al. Safflower (Carthamus tinctorius L.) seed attenuates memory impairment induced by scopolamine in mice via regulation of cholinergic dysfunction and oxidative stress. Food Funct 2019;10(6):3650-59.

16. Wei QS, Hong GJ, Yuan YJ, Chen ZQ, Zhang QW, He W. Huo Xue Tong Luo capsule, a vasoactive herbal formula prevents progression of asymptomatic osteonecrosis of femoral head: A prospective study. J Orthop Transl 2019;18:65-73.

17. Fang B, Li Y, Chen C, Wei QS, Zheng JQ, Liu YM, et al. Huo Xue Tong Luo capsule ameliorates osteonecrosis of femoral head through inhibiting lncRNA-Miat. J

Ethnopharmacol 2019;238.

18. Ao H, Feng W, Peng C. Hydroxysafflor Yellow A: A Promising Therapeutic Agent for a Broad Spectrum of Diseases. Evid Based Complement Alternat Med 2018;2018:8259280.

19. Ma L, Liu L, Ma Y, Xie H, Yu X, Wang X, et al. The Role of E-Cadherin/beta-Catenin in Hydroxysafflor Yellow A Inhibiting Adhesion, Invasion, Migration and Lung Metastasis of Hepatoma Cells. Biol Pharm Bull 2017;40(10):1706-15.

20. Zhu HJ, Wang LJ, Wang XQ, Pan H, Li NS, Yang HB, et al. Hydroxysafflor yellow A (HYSA) inhibited the proliferation and differentiation of 3T3-L1 preadipocytes. Cytotechnology 2015;67(5):885-92.

21. Hu ZC, Xie ZJ, Tang Q, Li XB, Fu X, Feng ZH, et al. Hydroxysafflor yellow A (HSYA) targets the NF-κB and MAPK pathways and ameliorates the development of osteoarthritis. Food Funct 2018;9(8):4443-56.

22. Lv MY, Shi CJ, Pan FF, Shao J, Feng L, Chen G, et al. Urolithin B suppresses tumor growth in hepatocellular carcinoma through inducing the inactivation of Wnt/β-catenin signaling. Journal of cellular biochemistry 2019;120(10):17273-82.

23. Fang B, Wang D, Zheng J, Wei Q, Zhan D, Liu Y, et al. Involvement of tumor necrosis factor alpha in steroid-associated osteonecrosis of the femoral head: friend or foe? Stem cell research & therapy 2019;10(1):5.

24. Hamburger V, Hamilton HL. A series of normal stages in the development of the chick embryo. 1951. Dev Dyn 1992;195(4):231-72.

25. Schmitz N, Laverty S, Kraus VB, Aigner T. Basic methods in histopathology of joint

tissues. Osteoarthritis Cartilage 2010;18 Suppl 3:S113-6.

26. Li Y, He X, Li Y, He J, Anderstam B, Andersson G, et al. Nicotinamide phosphoribosyltransferase (Nampt) affects the lineage fate determination of mesenchymal stem cells: a possible cause for reduced osteogenesis and increased adipogenesis in older individuals. Journal of bone and mineral research : the official journal of the American Society for Bone and Mineral Research 2011;26(11):2656-64.

27. Xu L, Huang S, Hou Y, Liu Y, Ni M, Meng F, et al. Sox11-modified mesenchymal stem cells (MSCs) accelerate bone fracture healing: Sox11 regulates differentiation and migration of MSCs. Faseb J 2015;29(4):1143-52.

28. Li CJ, Cheng P, Liang MK, Chen YS, Lu Q, Wang JY, et al. MicroRNA-188 regulates age-related switch between osteoblast and adipocyte differentiation. The Journal of clinical investigation 2015;125(4):1509-22.

29. Muruganandan S, Govindarajan R, Sinal CJ. Bone Marrow Adipose Tissue and Skeletal Health. Curr Osteoporos Rep 2018;16(4):434-42.

30. Jules J, Chen W, Feng X, Li YP. CCAAT/Enhancer-binding Protein α (C/EBPα) Is Important for Osteoclast Differentiation and Activity. J Biol Chem 2016;291(31):16390-403.

31. Chen W, Zhu G, Tang J, Zhou HD, Li YP. C/ebpα controls osteoclast terminal differentiation, activation, function, and postnatal bone homeostasis through direct regulation of Nfatc1. The Journal of pathology 2018;244(3):271-82.

32. Orimo H. The mechanism of mineralization and the role of alkaline phosphatase in health and disease. Journal of Nippon Medical School = Nippon Ika Daigaku zasshi

2010;77(1):4-12.

33. Molagoda IMN, Karunarathne W, Choi YH, Park EK, Jeon YJ, Lee BJ, et al. Fermented Oyster Extract Promotes Osteoblast Differentiation by Activating the Wnt/beta-Catenin Signaling Pathway, Leading to Bone Formation. Biomolecules 2019;9(11).

34. Lerner UH, Ohlsson C. The WNT system: background and its role in bone. J Intern Med 2015;277(6):630-49.

35. Pan MR, Hsu MC, Chen LT, Hung WC. G9a orchestrates PCL3 and KDM7A to promote histone H3K27 methylation. Scientific reports 2015;5:18709.

36. Tsukada Y, Ishitani T, Nakayama KI. KDM7 is a dual demethylase for histone H3 Lys 9 and Lys 27 and functions in brain development. Genes & development 2010;24(5):432-7.

37. Wang L, Xu S, Lee JE, Baldridge A, Grullon S, Peng W, et al. Histone H3K9 methyltransferase G9a represses PPARgamma expression and adipogenesis. EMBO J 2013;32(1):45-59.

38. Liu L, Tao W, Pan W, Lici L, Yu Q, Zhang D, et al. Hydroxysafflor Yellow A Promoted Bone Mineralization and Inhibited Bone Resorption Which Reversed Glucocorticoids-Induced Osteoporosis. Biomed Res Int 2018;2018.

Figures and legends

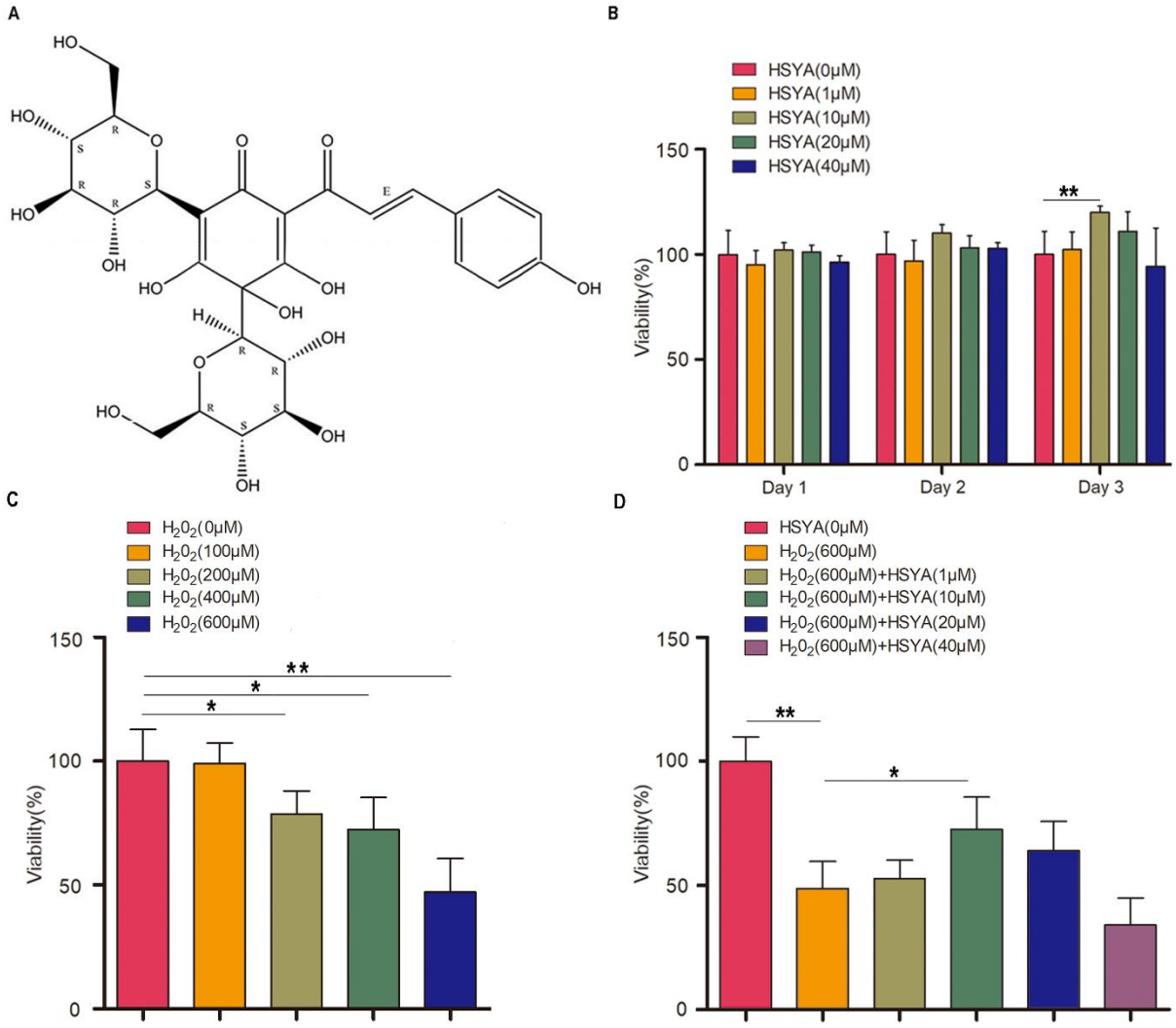

Fig. 1 Viability of hBMSCs treated by HSYA at different concentrations. (A) The basic chemical structure of HSYA. (B) The cells were incubated with HSYA (0, 1, 10, 20, 40μM) for 1, 2 and 3 days, and then CCK-8 assay was performed to test the cell viability. ***p*<0.01, n=6. (C) BMSCs were treated with H_2O_2 (0-600 μM) for 2 h, then the cell viability was measured. **p*<0.05, ***p*<0.01, n=6. (D) BMSCs were treated with H_2O_2 (0-600 μM) for 2 h, then HSYA (0, 1, 10, 20, 40μM) was added into the plate and cultured for a further 24h before the test. **p*<0.01, ***p*<0.01, n=6.

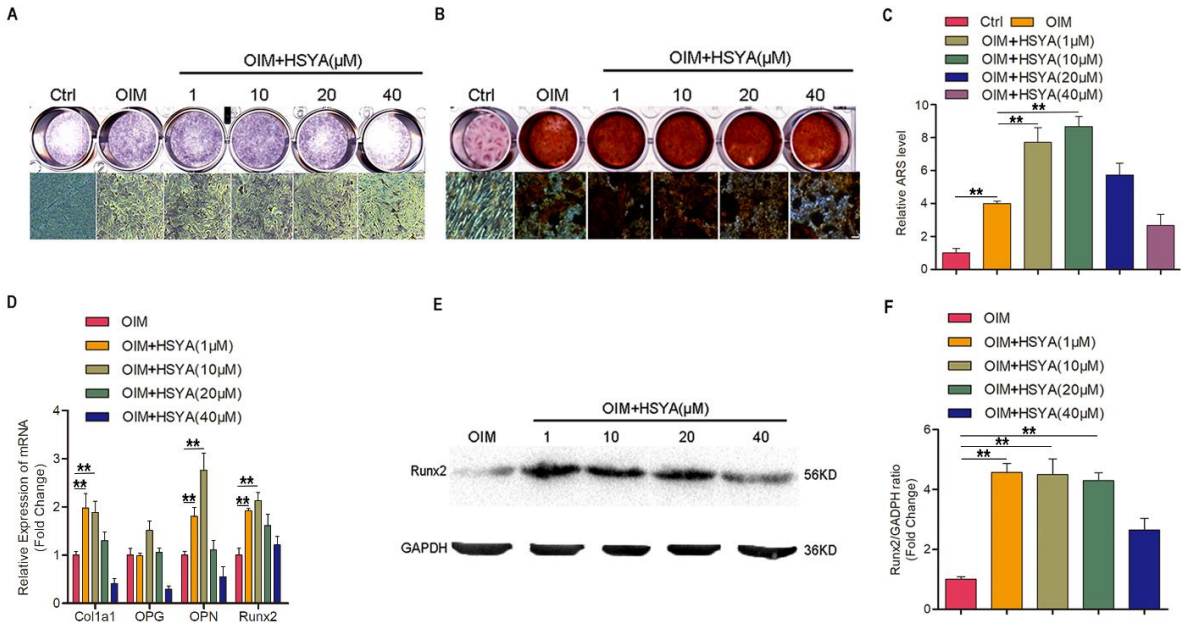

Fig. 2 HSYA promoted osteogenesis of hBMSCs. (A) hBMSCs were treated with OIM with or without HSYA (1, 10, 20, 40μM) for 7 days (A) or 14 days (B). Then the cells were fixed and stained with BCIP/NBT alkaline phosphatase coloration kit (A) or Alizarin Red S (B). (C) Quantification of Alizarin Red S staining of hBMSCs incubated with different concentrations of HSYA in OIM for 14 days. $^{**}p<0.01$, n=6. (D) hBMSCs were treated with HSYA (1, 10, 20, 40μM) in OIM for 7 days, then gene expressions were detected by real time PCR. β-actin was used as an internal control. $^{**}p<0.01$, n=6. (E) Representative western blot image of Runx2 at 7 day treated with OIM or HSYA (1, 10, 20 and 40μM) in OIM. (F) Relative quantification of the normalized expression of Runx2 against GAPDH as determined by Image J. $^{**}p<0.01$, n=3.

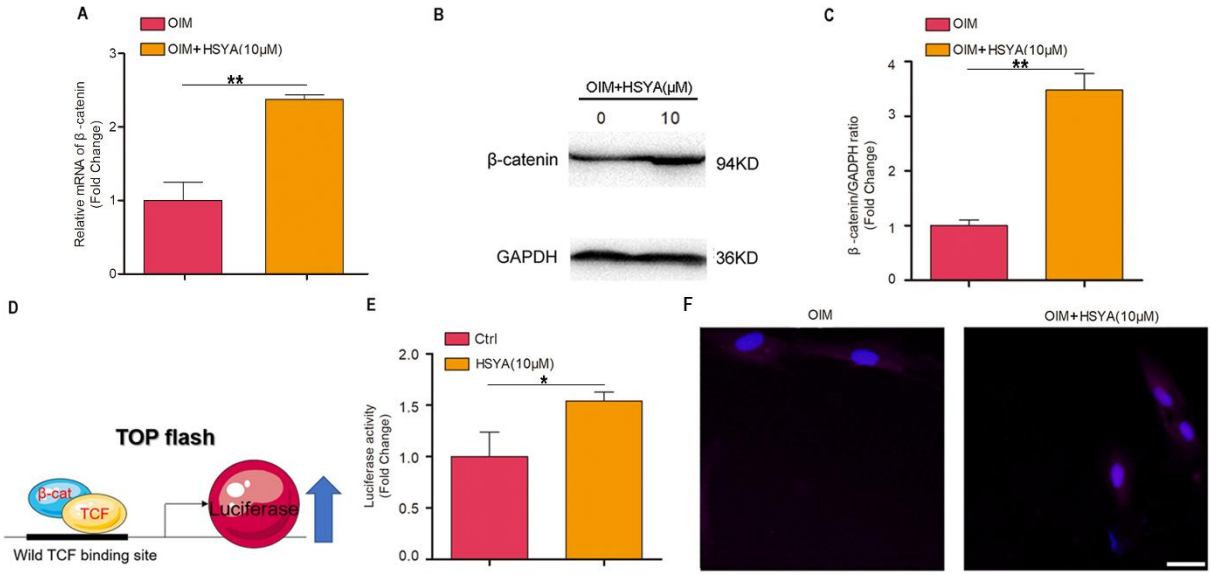

Fig. 3 HSYA regulated β-catenin expression in hBMSCs by histone demethylation. (A) hBMSCs were treated with HSYA (10 μM) in OIM for 7 days, then mRNA level of β-catenin was detected by real time PCR. β-actin was used as an internal control. ***p*<0.01, compared with OIM group, n=3. (B&C) Total proteins were extracted from hBMSCs at 7 day treated with OIM or HSYA (10 μM) in OIM, the expression level of β-catenin was detected by western blot. GAPDH was used as an internal control. Relative level of β-catenin was normalized by GAPDH and quantified by Image J. **p<.01 for statistical significance. (D&E) The TOPflash luciferase activity was measured in hBMSCs after treatment of HSYA at different concentrations. **p*<0.05, compared with Ctrl group, n=3. (F) Typical image of immunofluorescence staining of β-catenin incubated with 10μM HSYA in OIM for 24h. Scale bars=200 μm.

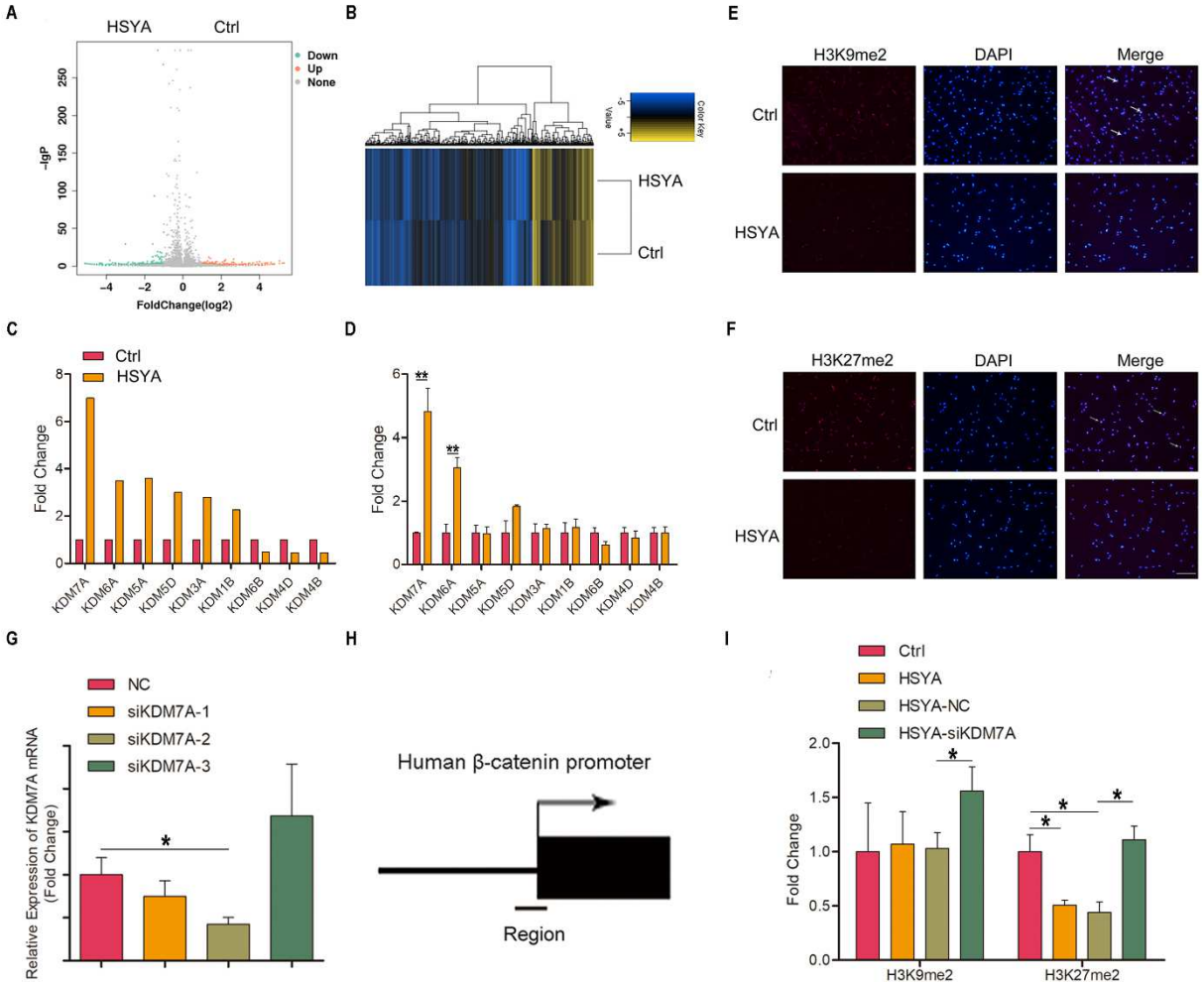

Fig. 4 HSYA activated β-catenin expression via histone demethylation. (A-D) HSYA regulated the expression of KDMs genes. (A) Heatmap depicting expression levels of genes between PBS- and HSYA-treated hBMSCs. (B) Volcano map of the differentially expressed genes in PBS- and HSYA-treated hBMSCs. (C) Relative level of human KDMs genes in PBS- and HSYA-treated hBMSCs as analyzed by RNA-seq. (D) Evaluate the expression levels of KDMs in PBS- and HSYA-treated hBMSCs by quantitative RT-PCR (n=3). β-actin was used as an internal control. $^{**}p<0.01$, compared with Ctrl group. (E&F) Typical image of immunofluorescence staining of H3K9me2&H3K27me2 incubated with 10μM HSYA in OIM for 48h. Scale bars=200 μm. (G) The siRNA targeting KDM7A was transfected into hBMSCs as mentioned in Methods and Materials. $^{*}p<0.05$ for statistical significance, compared with NC

group. (H) Schematical view of the promoter region of β-catenin detected by ChIP-PCR. (I) ChIP-PCR analysis of the occupancy of H3K9me2 and H3K27me2 on human β-catenin promoter. Normal rabbit IgG was used as loading control. *p<0.05 for statistical significance, compared with Ctrl group (n=3).

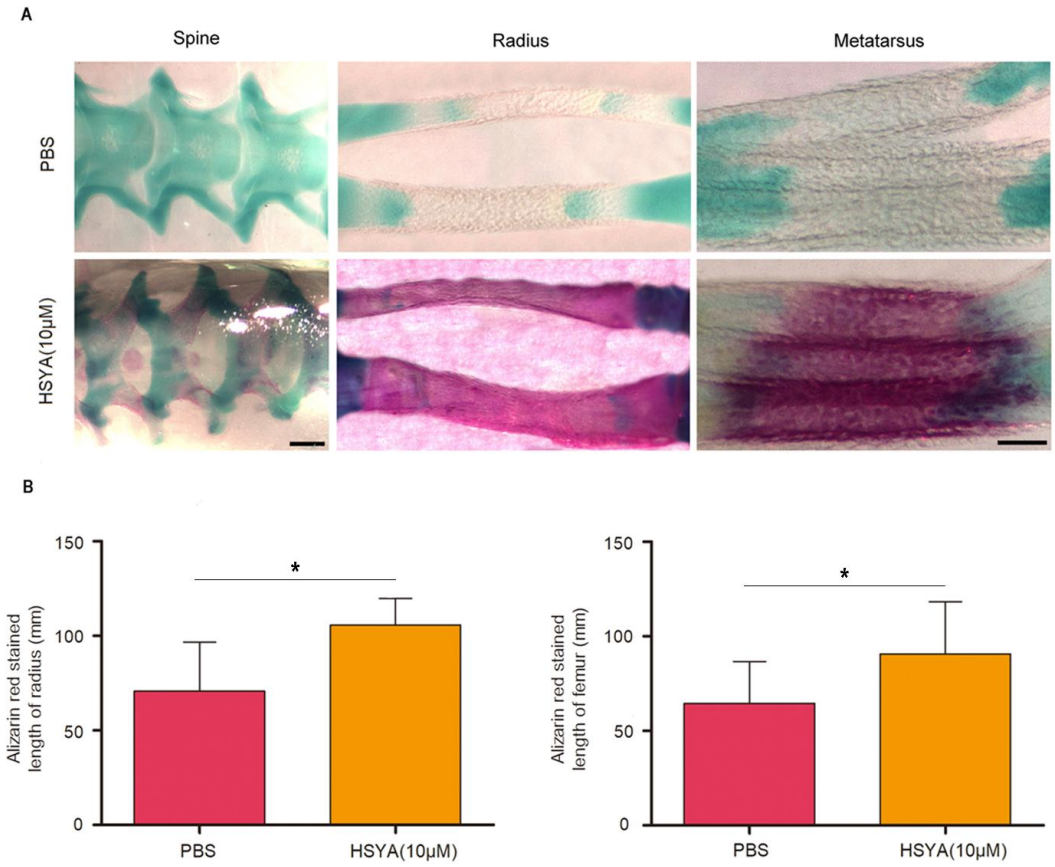

Fig. 5 HSYA exposure during gastrulation accelerated bone mineralization. (A) Representative appearance of chick embryos' spine, radius, metatarsus treated with PBS or 10μM HSYA. Scale bars=250 μm. (B) Bar charts comparing the length of alizarin red radius, and femur between PBS and HSYA-treated embryos. *p<0.05 for statistical significance, compared with PBS group (n=6). PBS: Phosphate-buffered saline.

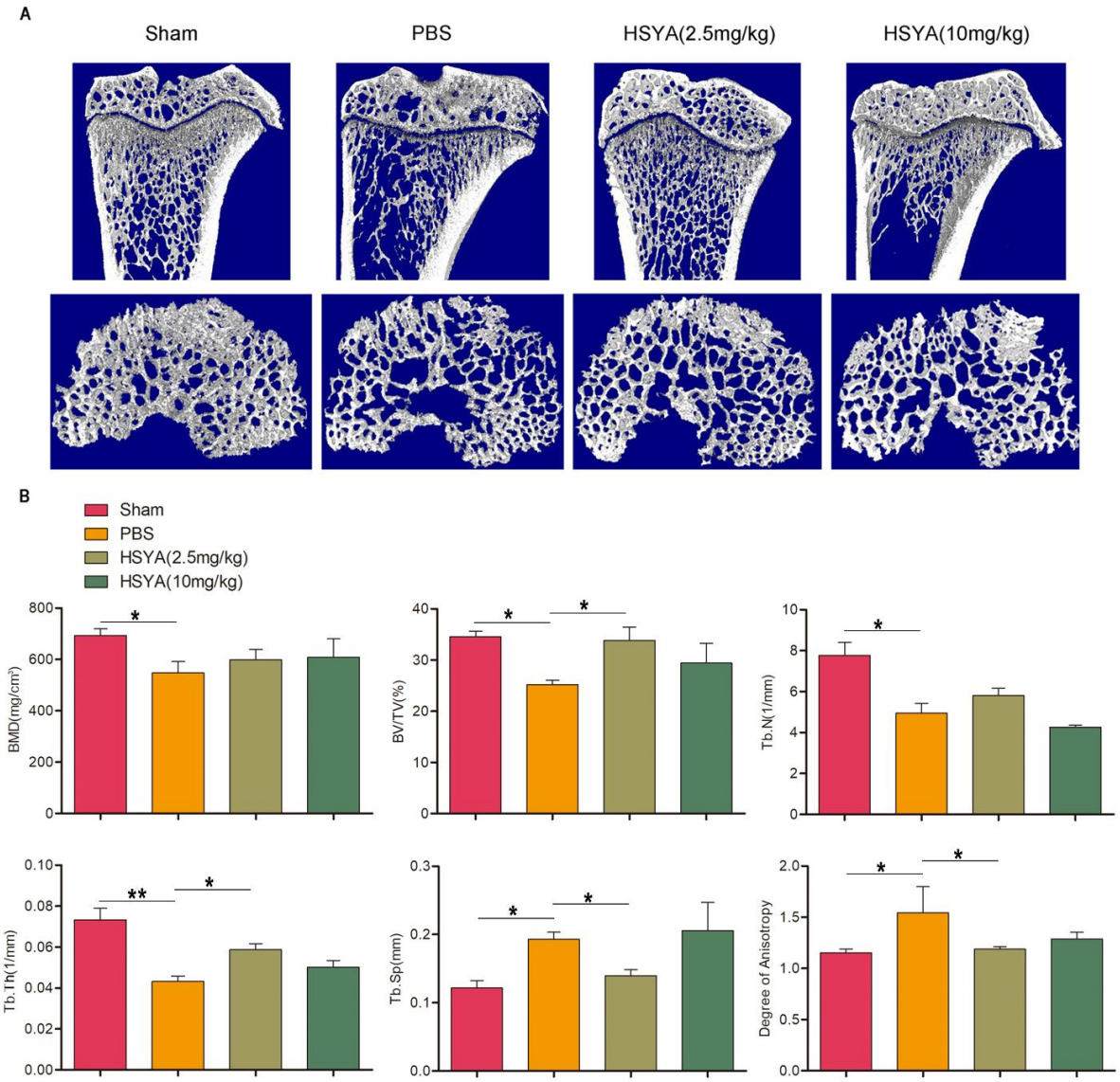

Fig. 6 HSYA prevented OVX-induced bone mass loss in vivo. (A) Representative 2-dimensional and 3-dimensional Micro-CT images of tibial growth plate in each group. (B) Quantitative analysis of parameters regarding to bone architecture, including BMD, BV/TV, Tb. N, Tb. Th, Tb. Sp (n=6). *P<0.05, **p<0.01.

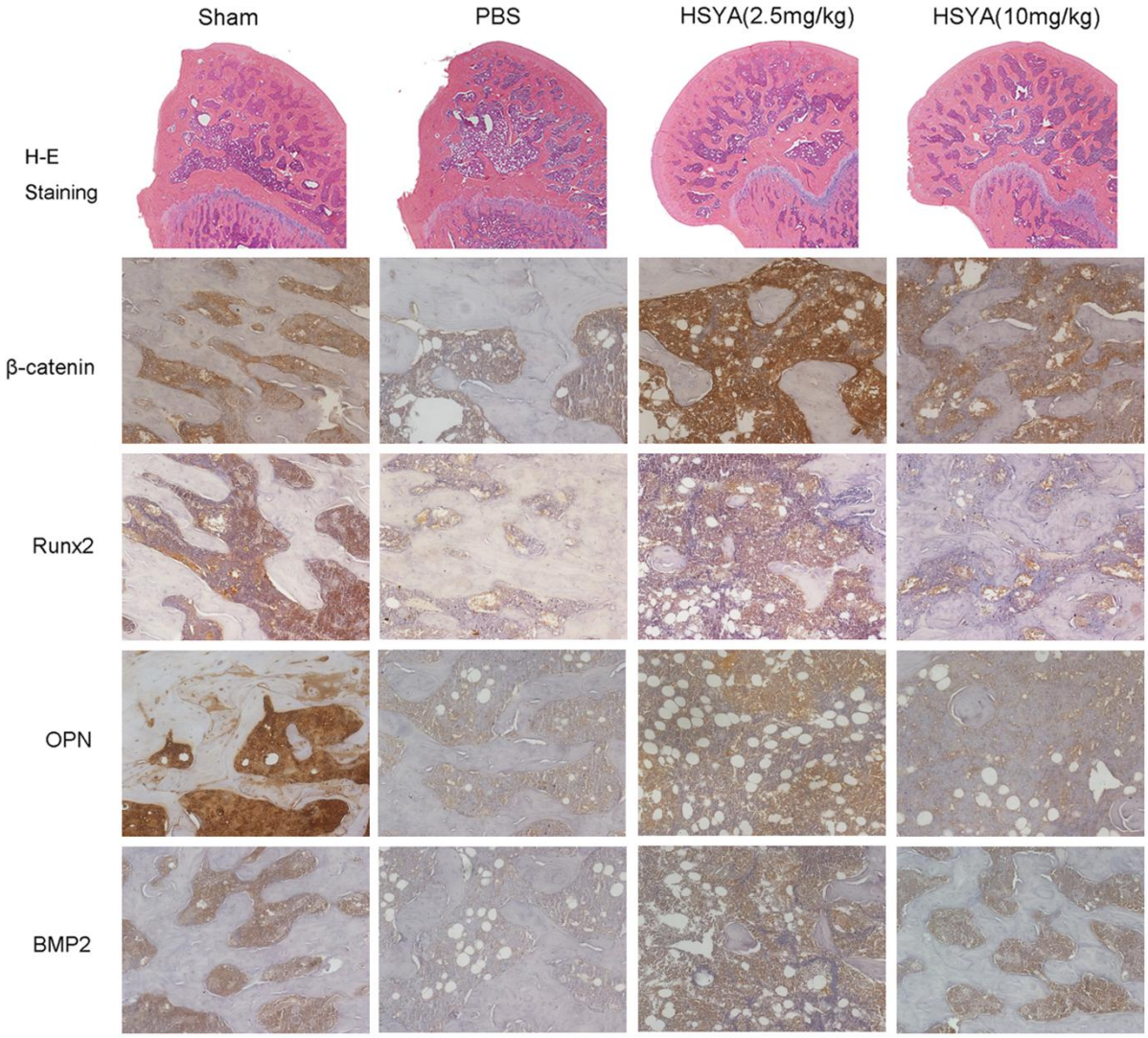

Fig. 7 HSYA improved the trabecular structure and stimulated the expression of osteogenic markers in OVX mice. Representative images of HE and immunohistochemical staining of distal femoral trabecular bone with indicated antibodies.

Supplementary files:

Supplementary Table 1. Sequences of primers for real time PCR analysis

Supplementary Table 2. Sequences of siRNAs targeting KDM7A

Data file S1. The changed genes in RNAseq data

Figures

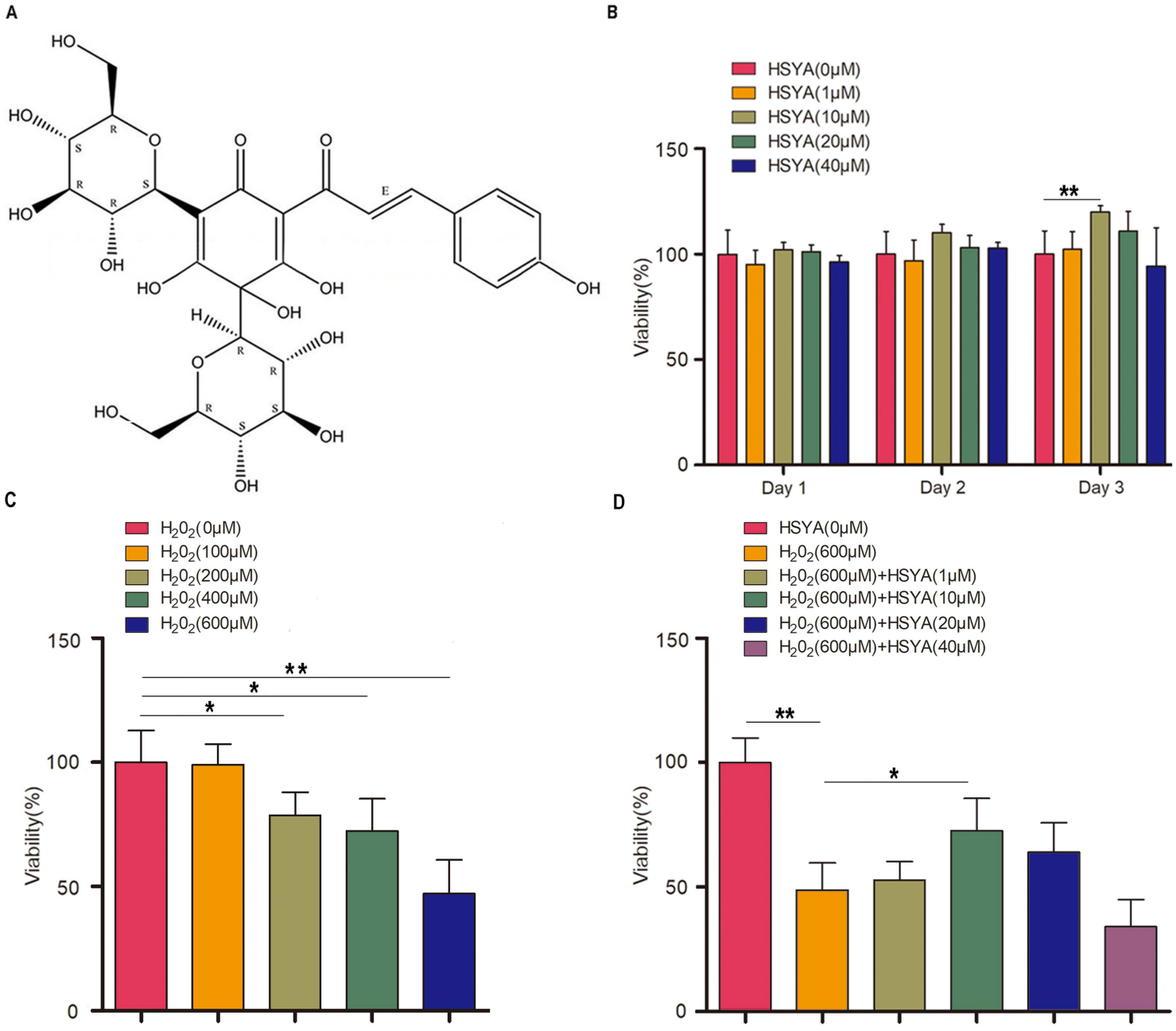

Figure 1

Viability of hBMSCs treated by HSYA at different concentrations. (A) The basic chemical structure of HSYA. (B)The cells were incubated with HSYA (0, 1, 10, 20, 40μM) for 1, 2 and 3 days, and then CCK-8 assay was performed to test the cell viability.**p<0.01, n=6.(C)BMSCswere treated with H2O2(0-600 μM) for 2 h,thenthe cell viability was measured.*p<0.05,**p<0.01, n=6.(D) BMSCswere treated with H2O2(0-600 μM) for 2 h,then HSYA(0, 1, 10, 20, 40μM)was added into the plate and cultured for a further24hbefore thetest.*p<0.01,**p<0.01, n=6

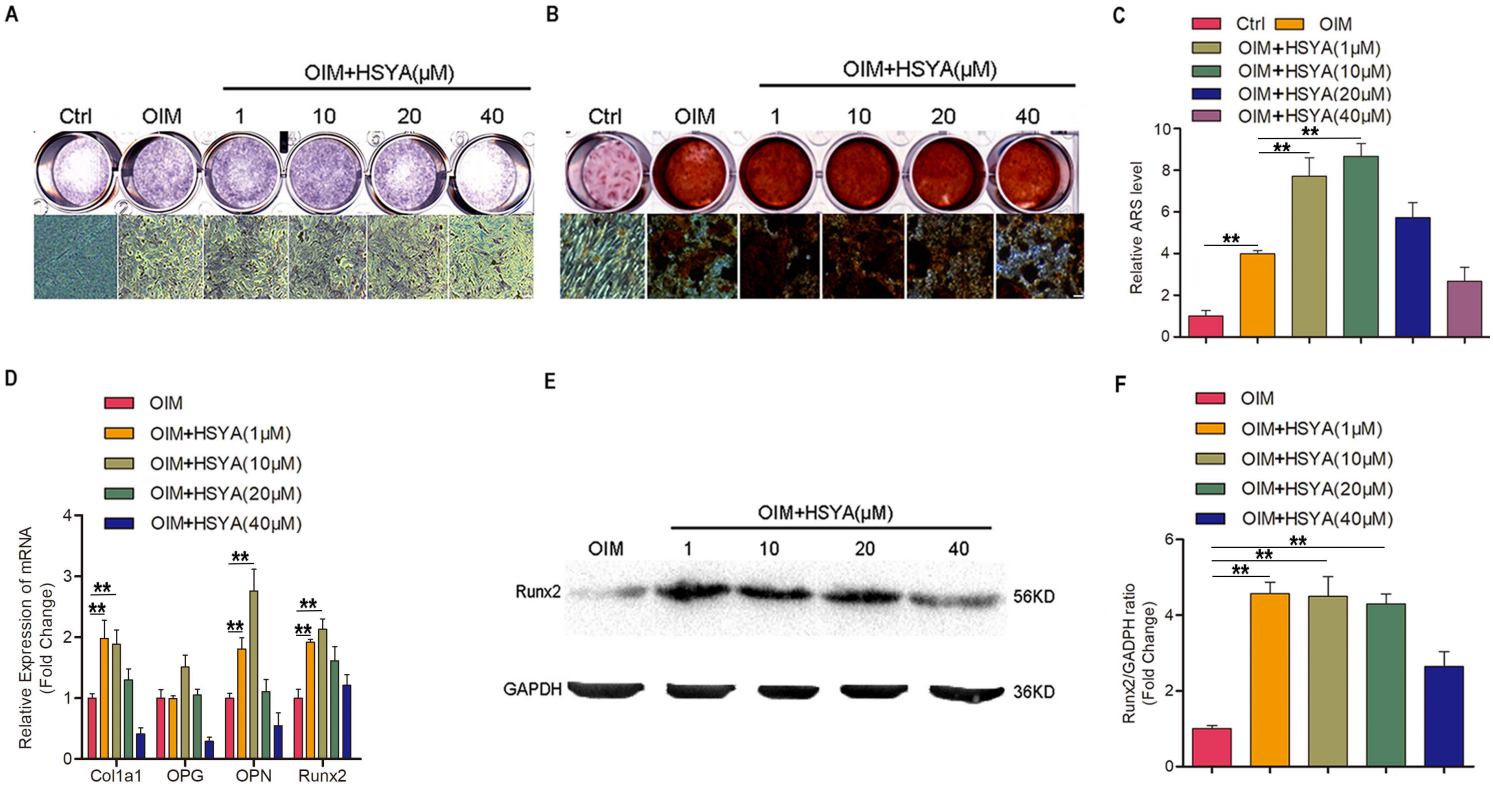

Figure 2

HSYA promotedosteogenesis of hBMSCs. (A)hBMSCs were treated withOIM with or without HSYA (1, 10, 20, 40μM) for 7 days (A) or 14 days (B). Then the cells were fixed and stained with BCIP/NBT alkaline phosphatase coloration kit (A) or Alizarin Red S(B). (C) Quantification ofAlizarin Red S staining of hBMSCs incubated with different concentrations of HSYA in OIM for 14 days.**p<0.01, n=6.(D)hBMSCs were treated with HSYA (1, 10, 20, 40μM) in OIM for 7 days, then gene expressions were detected by real time PCR. β-actin was used as an internal control. **p<0.01, n=6. (E) Representative western blot image of Runx2at 7 day treated with OIM or HSYA (1, 10, 20and 40μM) in OIM.(F)Relative quantification of the normalized expression of Runx2 against GAPDHasdetermined by Image J.**p<0.01, n=3

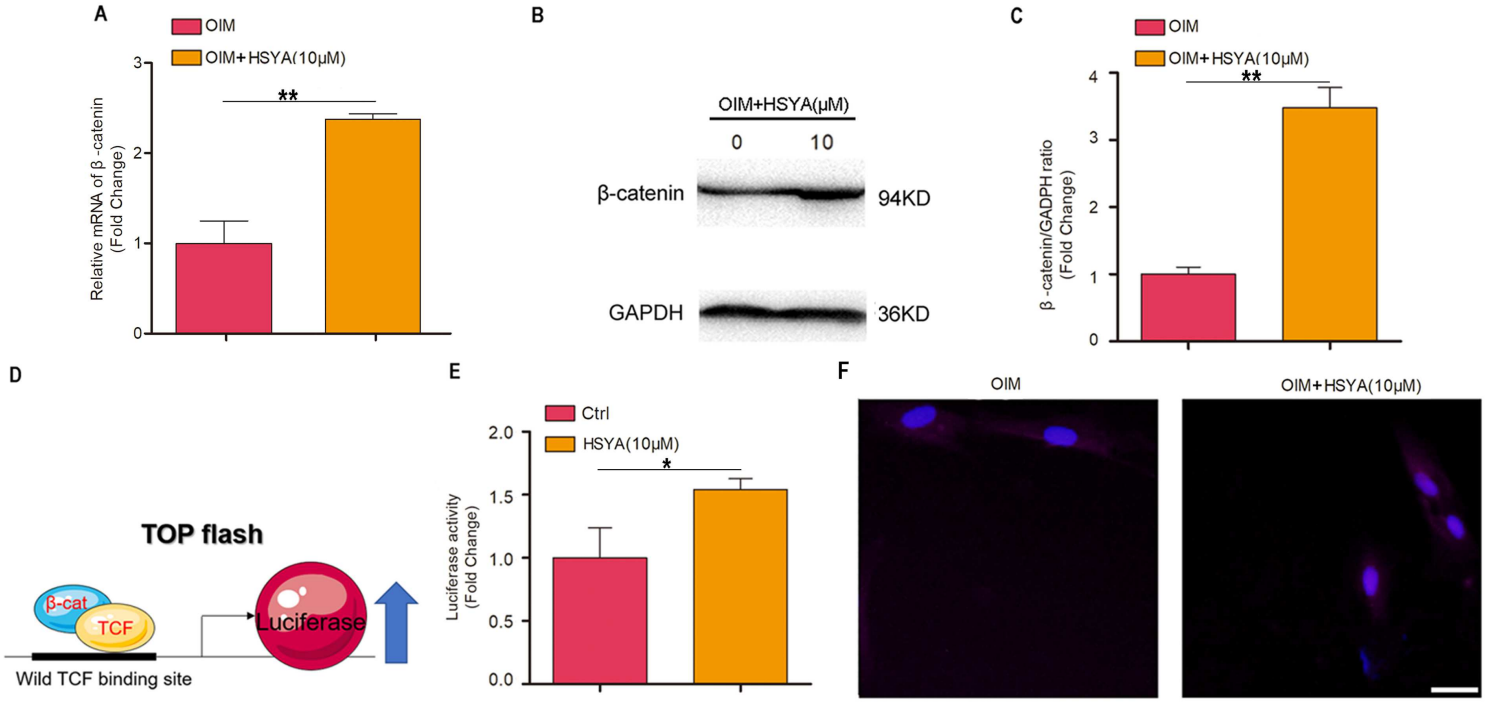

Figure 3

HSYA regulated β-catenin expression in hBMSCs by histone demethylation. (A)hBMSCs were treated with HSYA (10 μM) in OIM for 7 days, then mRNA level of β-cateninwasdetected by real time PCR. β-actin was used as an internal control. **p<0.01, compared with OIM group, n=3.(B&C) Total proteins were extracted from hBMSCs at 7 day treated with OIM or HSYA (10 μM) in OIM, the expression level of β-catenin was detected by western blot. GAPDH was used as an internal control.Relativelevelofβ-cateninwas normalized byGAPDHand quantified by Image J. **p<.01 for statistical significance.(D&E) The TOPflash luciferase activity was measured in hBMSCs after treatment of HSYA at different concentrations. *p<0.05, compared with Ctrl group, n=3.(F) Typical image of immunofluorescence staining of β-catenin incubated with 10μMHSYA in OIM for 24h.Scale bars=200 μm.

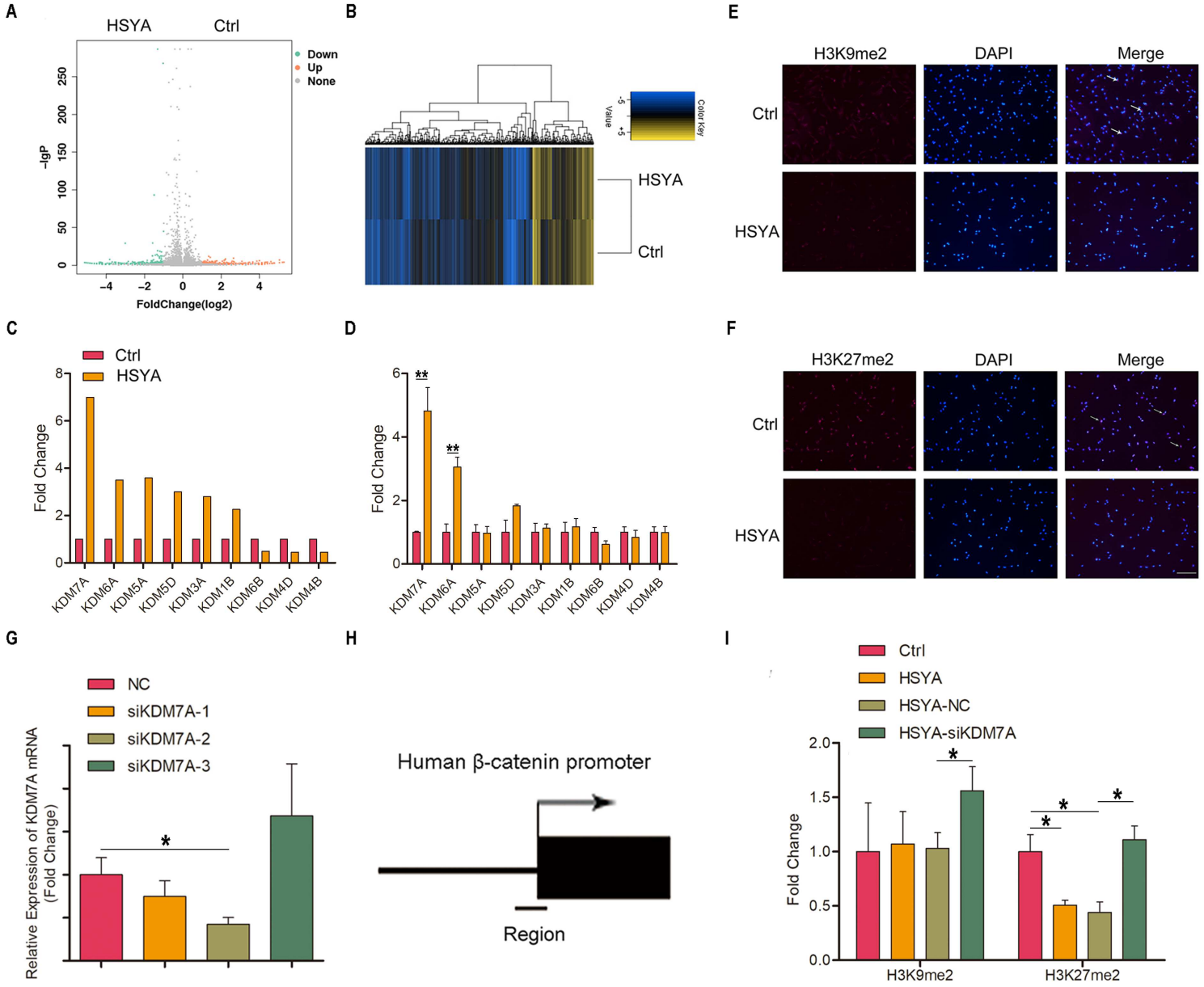

Figure 4

HSYA activated β-catenin expression via histone demethylation. (A-D) HSYA regulated the expression of KDMs genes.(A)Heatmap depicting expression levels of genes between PBS-and HSYA-treated hBMSCs. (B) Volcano map of the differentially expressed genes in PBS-and HSYA-treated hBMSCs. (C)Relative level of human KDMs genesin PBS-and HSYA-treated hBMSCs as analyzed by RNA-seq.(D) Evaluate the expression levels of KDMsin PBS-and HSYA-treated hBMSCsby quantitative RT-PCR (n=3). β-actin was used as an internal control. **p<0.01, compared with Ctrl group.(E&F)Typical image of immunofluorescence staining of H3K9me2&H3K27me2 incubated with 10μMHSYA in OIM for 48h.Scale bars=200 μm.(G) The siRNA targeting KDM7A was transfected into hBMSCs as mentioned in Methods and Materials. *p<0.05 for statistical significance, compared with NC group. (H) Schematical view of the promoter regionof β-catenindetected by ChIP-PCR. (I) ChIP-PCR analysis of the occupancy of H3K9me2 and H3K27me2 on human β-catenin promoter. Normal rabbit IgG was used as loading control. *p<0.05 for statistical significance, compared with Ctrl group (n=3).

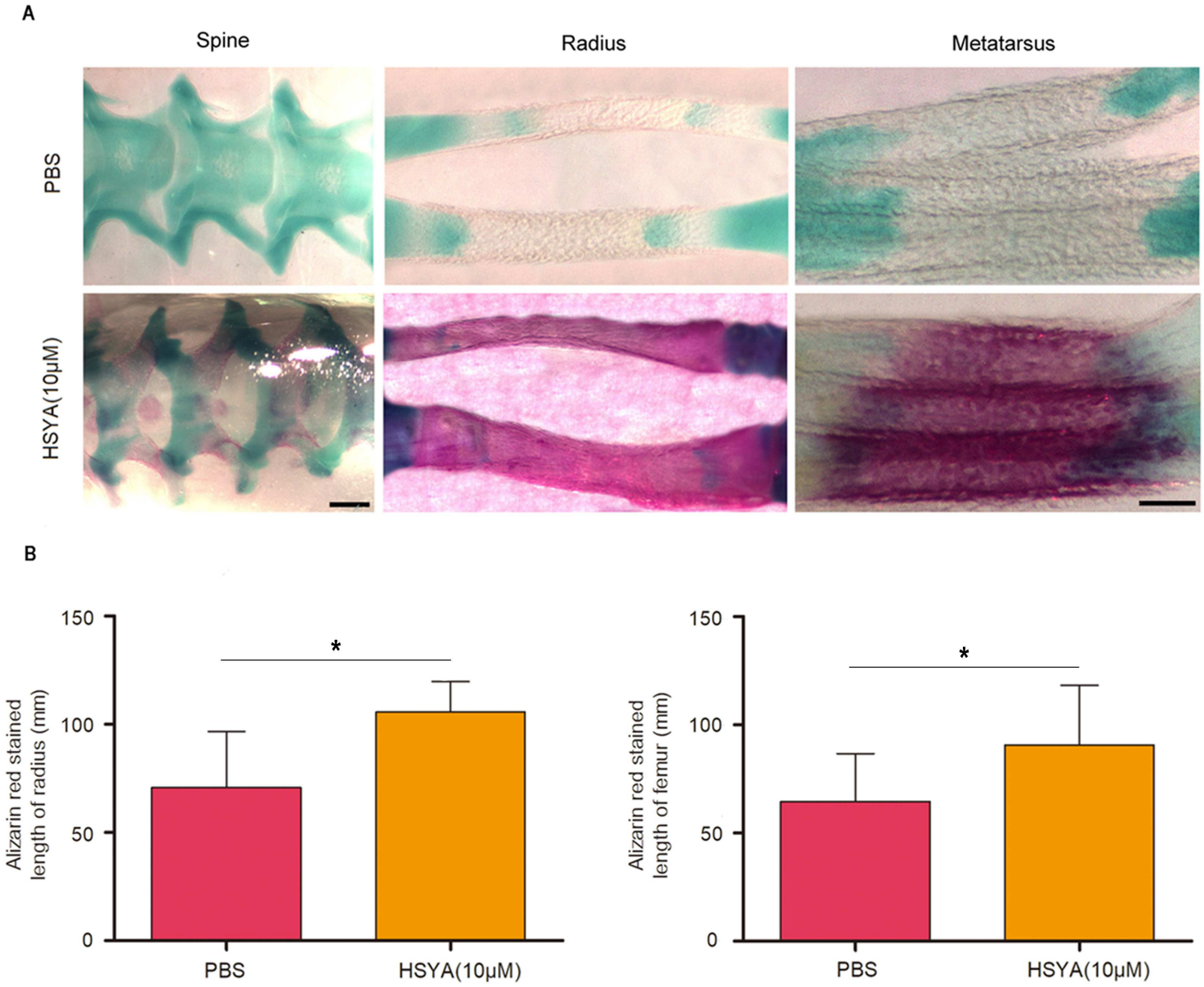

Figure 5

HSYA exposure during gastrulation acceleratedbone mineralization. (A) Representative appearance of chick embryos' spine, radius, metatarsus treated with PBS or 10μM HSYA. Scale bars=250 μm. (B) Bar charts comparing the length of alizarin red radius, and femur between PBS and HSYA-treated embryos. *p<0.05 for statistical significance, compared with PBS group (n=6). PBS: Phosphate-buffered saline.

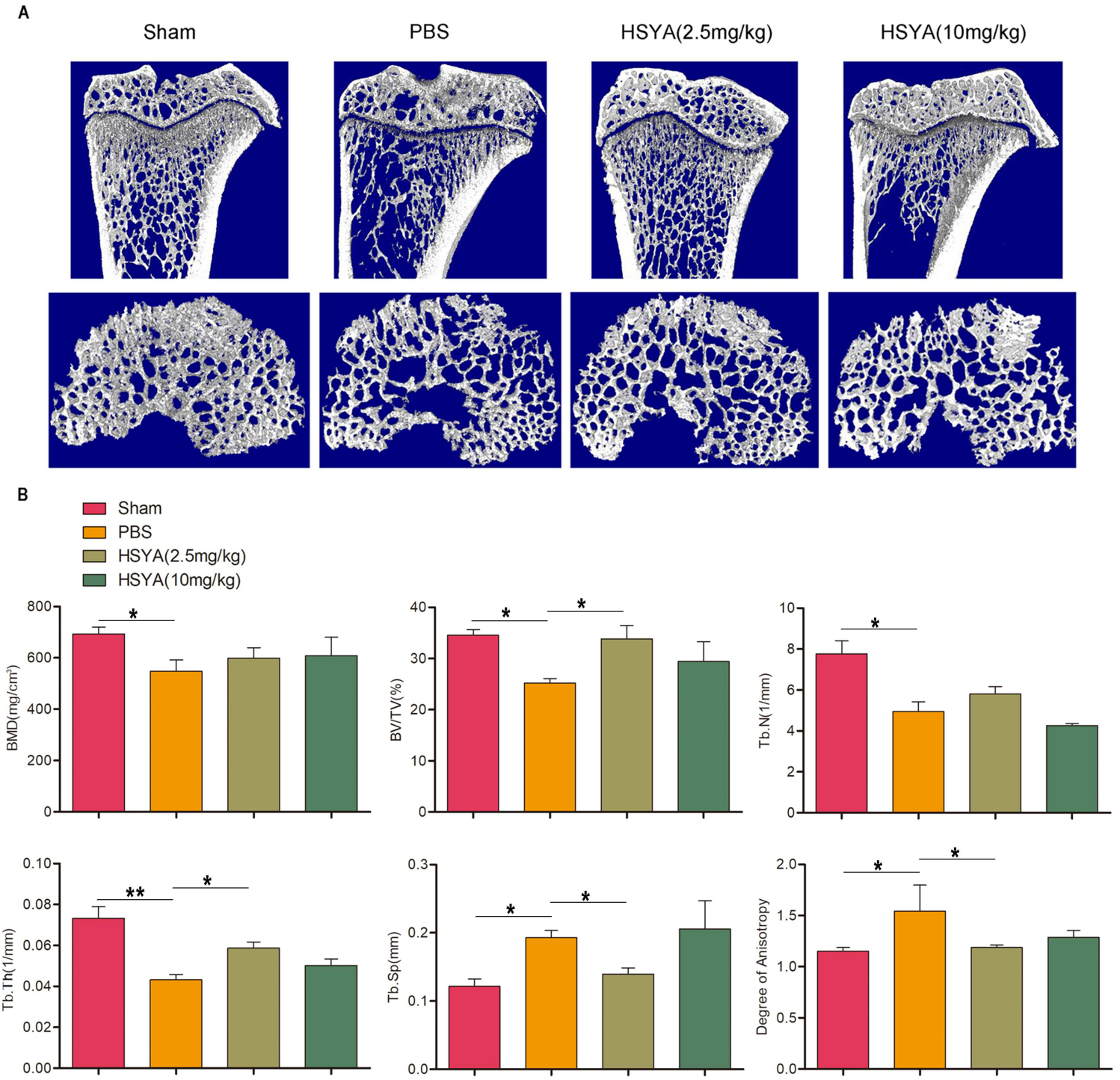

Figure 6

HSYA prevented OVX-induced bone mass loss in vivo. (A)Representative 2-dimensional and 3-dimensional Micro-CT images of tibial growth plateineach group.(B)Quantitative analysis of parameters regarding to bone architecture, including BMD, BV/TV, Tb. N, Tb. Th, Tb. Sp (n=6). *P<0.05, **p<0.01.

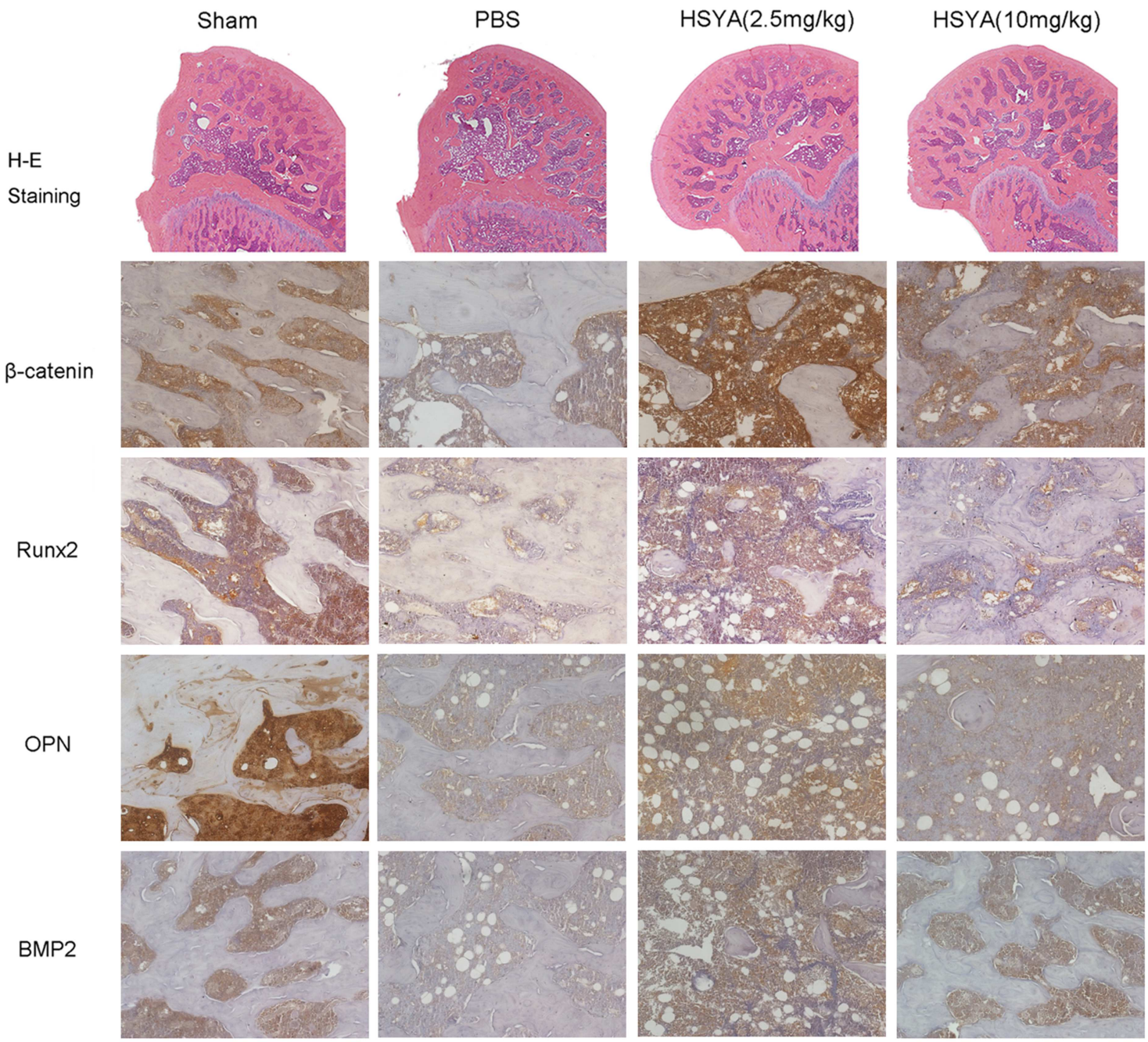

Figure 7

HSYA improved the trabecular structure and stimulated the expression of osteogenic markersin OVX mice.Representative images of HE and immunohistochemical staining of distal femoral trabecular bonewith indicated antibodies.